Journal of Advances in Biology & Biotechnology
2(2): 109-122, 2015; Article no.JABB.2015.013

SCIENCEDOMAIN *international*
www.sciencedomain.org

Identification of microRNAs Involved in mTOR Nutrient Signaling during Adipocyte Differentiation

Theresa Kaeuferle[1*], Andrea Osswald[1,2], Katrin K. Fleischmann[1], Philipp Pagel[3], Julia V. Frowein[1], Susanne Krauss-Etschmann[1,4] and Adelbert A. Roscher[1]

[1]Dr. von Hauner'sche Kinderklinik, Klinikum der Universität München, 80337 Munich, Germany.
[2]Medizinische Klinik und Poliklinik IV, Klinikum der Universität München, 80336 Munich, Germany.
[3]Department of Genome Oriented Bioinformatics, Technische Universität München, Wissenschaftszentrum Weihenstephan, 85354 Freising, Germany.
[4]Comprehensive Pneumology Center, Helmholtz Zentrum München, Ludwig-Maximilians Universität, member of the German Center for Lung Research (DZL) and Asklepios Clinic Gauting, 81377 Munich, Germany.

Authors' contributions

This work was carried out in collaboration between all authors. Authors AAR and SKE designed the study.Authors TK, AO, KKF and JVF performed the experiments. Author PP carried out the statistical analysis of microarrays and performed in silico target prediction; author TK wrote the first draft of the manuscript. Authors AAR, SKE, KKF and JVF edited manuscript. All authors read and approved the final manuscript.

Article Information

DOI: 10.9734/JABB/2015/14250
Editor(s):
(1) Csilla Tothova, Clinic for Ruminants, University of Veterinary Medicine and Pharmacy in Kosice, Slovak Republic.
Reviewers:
(1) Ng Zhi Xiang, Department of Biomedical Science, Faculty of Medicine, MAHSA University, Malaysia.
(2) Anonymous, University of Palermo, Italy.
Complete Peer review History: http://www.sciencedomain.org/review-history.php?iid=875&id=39&aid=7373

Original Research Article

Received 24th September 2014
Accepted 30th October 2014
Published 17th December 2014

ABSTRACT

Aims: In this study, we specifically aimed at identifying distinct miRNAs that are governing nutrient-driven adipogenesis *via* the mTOR pathway.
Methodology: The murine pre-adipocyte cell line 3T3-L1 was differentiated in the presence and absence of mTOR inhibitor rapamycin. MiRNA profiles were generated using two different array platforms. Differential regulated miRNAs were subjected to *in silico* target prediction. Candidate miRNA-target pairs were studied *via* luciferase assays, transfection assays and functional assays.
Results: This study confirmed 31 previously known and revealed 7 additional miRNAs, namely miR-

**Corresponding author: E-mail: Theresa.Kaeuferle@med.uni-muenchen.de;*

34a, -96, -106b, -148b, -214*, -678 and -690 as being involved in adipocyte differentiation. Furthermore, we identified a subset of 16 miRNAs showing both responsiveness to rapamycin and being predicted to target genes within the mTOR pathway. Within mTOR signaling, the novel miRNA-target pairs miR183-*Tsc1* (tuberous sclerosis 1), miR378-*Tsc1* and miR103-*Pik3r1* (phosphatidylinositol 3-kinase regulatory subunit alpha), were confirmed *via* luciferase-based binding assays. Accordingly we observed down-regulation of *Tsc1* on transcript level in cells transfected with miR-183 or -378 (18.3 % *P* = .004 and 40.4 % P < .0001). However, on protein level we could detect Tsc1 up-regulation (35.7 % and 39.8 %), which is consistent with an inhibitory influence on mTOR signaling (33.6 % and 32.9 %) and on adipocyte differentiation of these miRNAs.

Conclusion: Our findings reveal a novel role for a set of miRNAs during adipocyte differentiation and mTOR signaling. Especially the attenuating effect of miR-183 and -378 on adipocyte differentiation and mTOR signaling suggests their potential as biomarkers for nutrient-driven dysregulation of adipogenesis.

Keywords: microRNA; mTOR; adipocyte differentiation; Tsc1; nutrient signaling.

ABBREVIATIONS

Delta-like 1 homolog (Dlk1); mammalian target of rapamycin (mTOR); phosphatidylinositol 3-kinase regulatory subunit alpha (Pik3r1); phosphatidylinositol 3-kinase regulatory subunit gamma (Pik3r3); Peroxisome proliferator-activated receptor gamma (Pparγ); peptidylprolyl isomerase b (Ppib); pre-adipocyte factor-1 (Pref-1); p70 ribosomal protein S6 kinase (Rps6kb); p70 ribosomal protein S6 kinase 1 (S6k1); Tuberous sclerosis 1 (Tsc1).

1. INTRODUCTION

Understanding the molecular basis of nutrient-driven adipogenesis is essential to identify and monitor new therapeutics, either by drugs or diets that could ameliorate the adverse sequels of obesity. Various nutrient-signaling pathways are responsible for adapting protein synthesis, cell growth and cell differentiation to nutrient availability towards maintenance of whole-body metabolic homeostasis [1]. Among these, the mechanistic target of rapamycin (mTOR) pathway is an evolutionary conserved and well-studied intracellular nutrient-signaling pathway involved in the regulation of adipocyte differentiation, lipogenesis and intracellular accumulation of triglycerides [2,3]. *In vivo* studies in humans showed that chronic nutrient overload activates mTOR signaling and leads to insulin resistance [4], whereas inhibiting TOR-signaling blocks metabolic and cardiotoxic phenotypes caused by high fat diet in *Drosophila* [5]. The key enzyme of this pathway is the protein kinase mTOR complex 1 which can be experimentally inhibited by rapamycin, thereby negatively affecting insulin signaling and adipocyte differentiation [3]. In clinical practice rapamycin (*alias* sirolimus) and its derivatives are mainly used in transplant patients for their immunosuppressive activity [6,7]. Its *in vivo* application in obese subjects for the purpose of inhibiting nutrient-driven mTOR overactivation and adipocyte differentiation is precluded by associated unfavorable side-effects [8-10]. However, the identification of the specific targets that exert rapamycin-like effects on nutrient signaling might provide an approach to search for alternative therapeutic options.

MiRNAs control gene expression post-transcriptionally and are known to play a role in lipid and lipoprotein metabolism [11]. By targeting few key regulatory molecules within a given pathway, single miRNAs can control whole signaling cascades [12]. Some specific miRNAs were shown to play a role in obesity and its associated pathologies [13-15]. This knowledge has been utilized to treat e.g. hypercholesterolemia and liver steatosis in mice [16]. Some miRNAs, such as miR-99a, -100 and -199a* have previously been implicated in mTOR nutrient signaling in the context of cancer and dermal wound healing [17-20]. However, the pattern of miRNA regulation involved in mTOR signaling during adipocyte differentiation has not yet been elucidated.

In this study, we specifically aimed at identifying distinct miRNAs that are associated with the inhibition of adipogenesis *via* the effect of rapamycin on mTOR nutrient signaling. Our findings reveal a novel role for a set of miRNAs

during adipocyte differentiation and mTOR signaling. Among 22 identified rapamycin sensitive miRNAs miR-183 and -378 appear to be functionally relevant in mTOR signaling and adipocyte differentiation.

2. MATERIALS AND METHODS

2.1 Differentiation of 3T3-L1 Pre-adipocytes

3T3-L1 and HEK-293 cells were pre-cultured in DMEM (4.5 g/l glucose, with L-Glutamine; PAA, Pasching, Austria) supplemented with 10% Fetal Bovine Serum (Invitrogen, Life Technologies, Carlsbad, CA, USA) and 1% antibiotic-antimycotic solution (PAA). Differentiation was initiated by the addition of 200 nM insulin (Aventis, Sanofi, Paris, France), 1 µM dexamethasone (Sigma-Aldrich, St. Louis, MO, USA) and 0.5 mM 3-isobutyl-1-methylxanthine (Fluka, Sigma-Aldrich) at day 0. After two days, cells were further grown in growth medium supplemented with 200 nM insulin. Subsequently, medium was changed every two days until cell harvest at day 8.

24 hours post transfection differentiation was initiated (designated as day 0) by the addition of 200 nM insulin, 1 µM dexamethasone and 0.5 mM IBMX to growth medium. After 3 days cells were further grown in growth medium supplemented with 200 nM insulin and medium was changed again at day 5. Cells were differentiated for 6 days before harvest.

2.2 Oil Red O staining

Oil Red O staining of 3T3-L1 cells was performed following the procedure described by Green and Kehinde [21] with minor modifications. Briefly, 3T3-L1 cells were washed with PBS and fixed in 0.5% glutaric acid solution (Sigma-Aldrich, St. Louis, MO, USA) for 5 min. Cells were washed twice with PBS followed by a wash step with 60% isopropanol. Cells were stained in fresh Oil Red O solution (60% 30.5 µM Oil Red O in isopropanol and 40% H_2O; Sigma Aldrich) for at least 1 h and washed with 60% isopropanol and PBS. Lipid deposition was evaluated optically by light microscopy (Leica DM IL, Leica, Wetzlar, Germany).

2.3 miRNA microarrays

For semiquantitative miRCURY™ Locked Nucleic Acid microRNA Arrays (miRCURY™ LNA Array, Exiqon, Vedbaek, Denmark), total RNA from 2 independent experiments was isolated at day 0 and day 8 from 3T3-L1 cells as described above and additionally purified by precipitation adding 10 µl ammonium acetate, 1 µl glycogen and 450 µl 100% ethanol per 100 µl RNA-solution, followed by incubation at -20°C overnight. Integrity of purified RNA was confirmed using an Agilent 2100 Bioanalyzer (Agilent Technologies, Santa Clara, CA, USA). Hy3-/Hy5 labeled RNA (miRCURY LNA microRNA Array Power Labeling Kit, Exiqon) was manually hybridized on miRNA microarrays (miRCURY™ LNA microRNA Array v9.2, Exiqon). Slides were scanned by a GenePix 4000A Microarray Scanner (Axon Instruments, Foster City, CA, USA) and analyzed by GenePix® Pro Software (Axon Instruments).

Quantitative miRNA profiles were generated *via* TaqMan® Array Rodent MicroRNA Cards (Applied Biosystems, Life Technologies, Carlsbad, CA, USA) according to the supplier's protocol, inclusive of preamplification steps. Total RNA from 1 experiment was prepared in an identical manner as for semiquantitative miRCURY™ LNA Arrays. TaqMan® LDA runs were performed on an ABI PRISM® 7900HT Fast Real-Time PCR System (Applied Biosystems) and analyzed by SDS v2.3 software (Applied Biosystems) employing the $\Delta\Delta C_T$-method [22]. Values were normalized using sno-202 as reference.

2.4 *In silico* target prediction

Prediction of direct miRNA targets was performed using five prediction programs: PITA, miRanda, targetScanS, pictar and targetspy. Targets with consensus target prediction of at least 2 algorithms were considered predicted. Because of the similarity of their seed sequences, miRNAs belonging to the same family were grouped. For enrichment analysis of rapamycin-sensitive miRNA target genes in specific pathways, DIANA-miRPath (v.1.0) software was used applying PicTar 4-way and TargetScan 5 algorithms [23].

2.5 Real-time PCR

MiRNA-levels were determined using TaqMan® MicroRNA Reverse Transcription Kit, TaqMan® Universal PCR Master Mix and TaqMan® MicroRNA Assays (Applied Biosystems) according to the manufacturer's instructions. Sno-202 levels were used for normalization [22]. Marker and target transcript levels were

determined using QuantiTect Reverse Transcription Kit (Qiagen) and Power SYBR® Green Mastermix (Applied Biosystems). Primers were designed using Primer3 (v. 4.0.0) [24]. *Ppib* was used for normalization. Relative quantification was analyzed by the $\Delta\Delta C_T$-method [22].

2.6 miRNA transfection assays

3T3-L1 cells were transfected with Pre-miR™ miRNA Precursor miRNAs, Anti-miR™ miRNA Inhibitors or the respective negative controls #1 (Ambion) using Lipofectamine 2000 (Invitrogen) according to the manufacturer's instruction. 72 hours post transfection target gene and protein levels were quantified.

2.7 Luciferase assays

PCR-amplified 3'UTRs of *Pik3r1*, *Pik3r3* and *Tsc1*were cloned into psiCHECK™-2 vector. HEK-293 cells were transfected with the Pre-miR™ miRNA Precursor miRNAs or negative control #1 (Ambion) and the respective vector constructs using Lipofectamine2000 (Invitrogen). After 48 h, *Renilla* luciferase activity was measured and normalized to firefly luciferase activity.

2.8 Immunoblot analysis

Protein was extracted from cells using TNT lysis buffer supplemented with Protease and Phosphatase Inhibitor Cocktails (Calbiochem®, Merck, Darmstadt Germany). 10 µg of protein was separated on a SDS-polyacrylamide gel and blotted on a PVDF membrane. The membrane immunoreacted with the respective antibodies against phosphorylated p70 S6 Kinase (Thr-389), p70 S6 Kinase, Tsc1 (Hamartin), PI3 Kinase p85 and α-tubulin. Bound HRP-linked secondary antibody was visualized by Immun-Star™ HRP Chemiluminescent Kit (BioRad, Hercules, USA). All antibodies were obtained from Cell Signaling, Danvers, USA.

2.9 Statistical analysis

For miRNA microarrays, statistical analysis was carried out with the data analysis and statistics language R (R Foundation for Statistical Computing)using the Bioconductor suite for bioinformatics [25], specifically the limma package [26].After background correction *via* the method of Ritchie et al. [27] non-positive spots were removed and the remaining signal intensity values were normalized to per-chip median values by loess-smoother normalization. Differential expression of microRNAs was analyzed with the limma package [28] fitting a linear model for each gene and computing a moderated *t*-statistic and its *P* value [26] and was shown as log of 'fold changes' ($Log_2FC=log_2$ expr1⁄expr2). *P* values were corrected for multiple testing by the method of Benjamini and Hochberg [29].

MiRNAs were designated as 'differentially regulated' if adj $P_{miRCURYTM\ LNA\ Array} < .05$ and $log_2FC_{TaqMan®\ LDA} \geq \pm 0.3$. Statistically significant differences of real-time PCR and reporter assay results were evaluated using Student's *t*-test provided in GraphPad Prism 5.0 (GraphPad Software, San Diego, CA, USA). *P* values of .05 or less were considered significant.

3. RESULTS

3.1 Strategy for miRNA Discovery and Confirmation

We aimed to generate a data set of differentiation-associated miRNAs whose expression is altered by mTOR. Therefore, we utilized the mTOR inhibitor rapamycin and compared miRNA profiles from 3T3-L1 cells undergoing a differentiation protocol over eight days in the presence or absence of rapamycin. To confirm a large number of miRNAs, which were significantly deregulated in semi-quantitative miRCURY™ LNA Array analysis, we used quantitative TaqMan® LDA arrays instead of single real-time PCRs. Results from miRCURY™ LNA Arrays and the quantitative TaqMan® LDA highly correlated (Spearman's Rho 0.80; *P*< 4.50e-16; Fig. 1).

MiRNAs were designated as 'differentially regulated' if they displayed concordant changes in both microarray platforms. We found 75 % of the miRNAs identified by miRCURY™ LNA Array in differentiation experiments and 79 % of the miRNAs during rapamycin treatment as being concordantly regulated in both microarray platforms. Unconfirmed miRNAs included 15 miRNAs, for which no probes were present on commercially available TaqMan LDA® and 4 miRNAs that showed divergent regulation. These were not considered for further analyses.

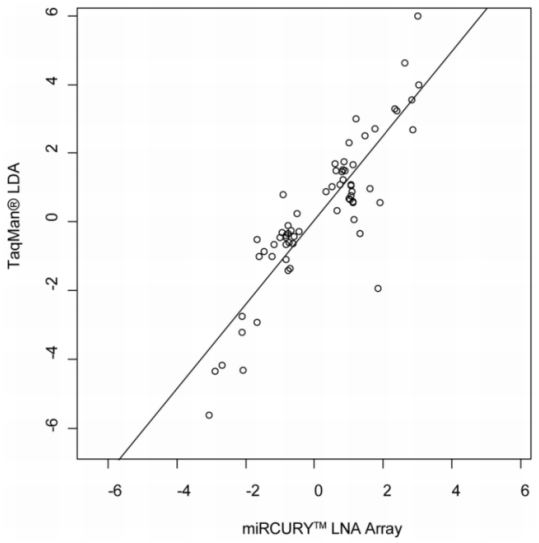

Fig. 1. Correlation between relative miRNA expression changes measured by TaqMan® LDA and miRCURY™ LNA Array analysis. Spots represent differential expression data (log_2 fold change of day 8 vs. day 0 and day 8 vs. day 8 of rapamycin treatment) of miRCURY™ LNA Array and TaqMan® LDA. MiRNAs which were differentially expressed during adipocyte differentiation andinhibition by rapamycin treatment are shown

Spearman's Rho = 0.80; P = 4.50e-16

3.2 Effect of rapamycin on adipocyte differentiation-associated miRNAs

Differentiation of 3T3-L1 pre-adipocytes (day 0) into adipocytes (day 8) was confirmed by increased levels of adipocyte marker transcript *Ppar-γ* (25-fold, *P*< .0001), decreased levels of pre-adipocyte marker transcript *Dlk1*, alias *Pref-1*, (11-fold, *P* < .0001) and by increasing deposition of lipid droplets (Fig. 2). Whereas *Ppar-y* expression increased continuously from day 2 to day 8, *Dlk1* levels decreased sharply in the initial phase of differentiation finally reaching the low levels of terminal differentiation. The strong up-/down-regulation of these biomarkers is reverted in adipocytes treated with 10 nM rapamycin. In concordance these cells resemble pre-adipocytes at an early stage of differentiation. Additionally, a markedly decreased cytoplasmic lipid droplet accumulation was observed (Fig. 2).

40 miRNAs fulfilled our criteria of showing confirmed differential regulation during adipocyte differentiation (Table s1). Among these, an involvement of miR-34a, -96, -106b, -148b, -214*, -678 and -690 in adipocyte differentiation has not been identified previously. Experiments utilizing the mTOR inhibitor rapamycin revealed 22 miRNAs as de-regulated between differentiated and rapamycin-treated adipocytes (Fig. 3). Among those, 18 miRNAs had already shown significant up- or down-regulation during differentiation, which was markedly attenuated or completely reverted by rapamycin. Four miRNAs did not change significantly during differentiation but were influenced by rapamycin (Fig. 3).

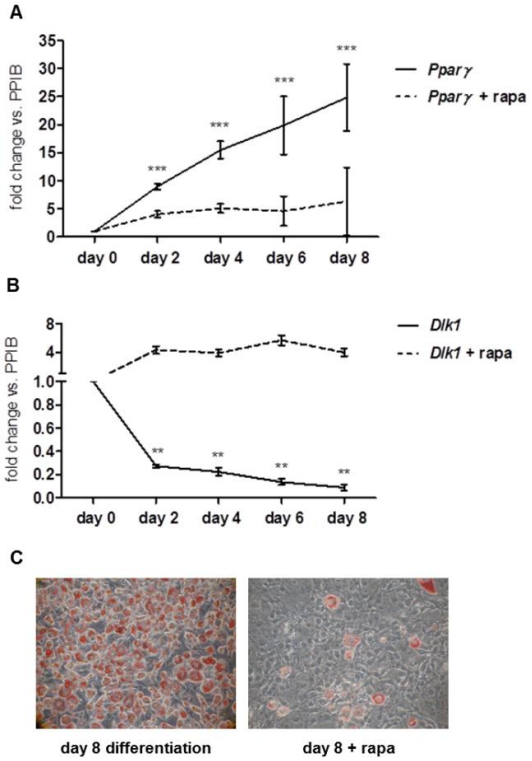

Fig. 2. Inhibitory effects of rapamycin on 3T3-L1 differentiation. (A) Real-time PCR mediated quantification of marker gene expression of adipocyte marker *Ppar-γ* and (B) Pre-adipocyte marker *Dlk1* (alias *Pref-1*) in differentiating adipocytes in the absence or presence of 10 nM rapamycin (+ rapa). Mean values ± S.E.M. of two experiments, each performed in triplicates. (C) Phenotypic comparison of untreated and rapamycin-treated cells undergoing a differentiation protocol for 8 days. Cells were fixed and stained with Oil Red O (200x magnification)

*Statistical significances were calculated between expression levels in the presence and absence of rapamycin at the respective time-points. ** P ≤ .01, *** P ≤ .001*

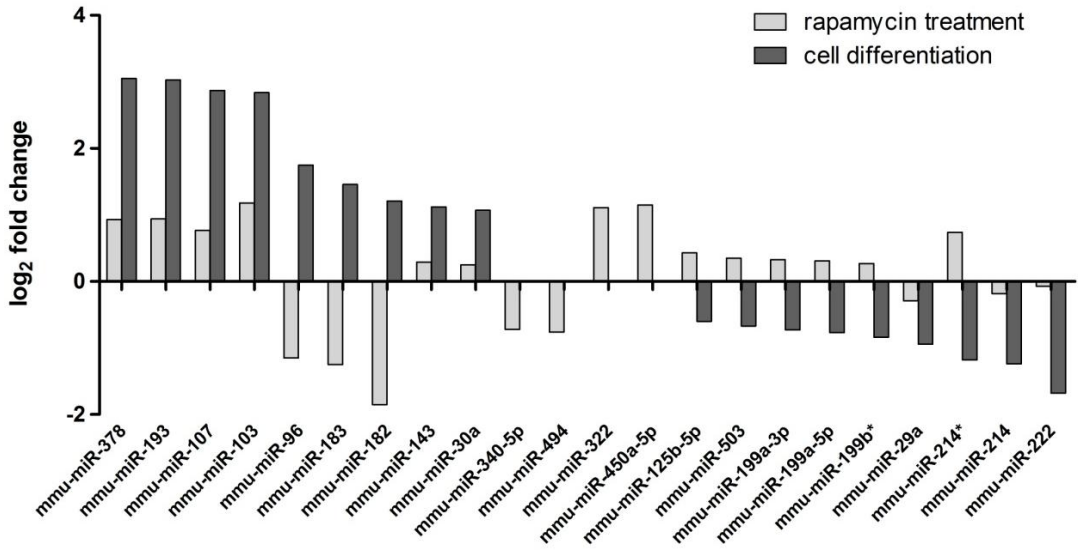

Fig. 3. Influence of rapamycin on miRNA expression during adipocyte differentiation

$Log_2FC_{miRCURY^{TM}\ LNA\ Array}$ values show miRNA expression changes between day 0 and day 8 of differentiating adipocytes in the absence (black) and in the presence of 10 nM rapamycin (grey). MiRNAs being confirmed as differentially expressed by both array platforms are shown

3.3 Predicted role of rapamycin-sensitive miRNAs within the mTOR pathway

Next we subjected the 22 rapamycin-sensitive miRNAs to a stringent *in silico* target prediction. From these, 16 miRNAs were concordantly predicted to target genes of the mTOR-pathway by at least two prediction tools (Table 1). Using DIANA-miRPath based enrichment analysis, we observed that *in silico* predicted targets for the set of rapamycin-sensitive miRNAs were significantly enriched in the mTOR pathway ($P_{\text{PicTar 4-way}}$ = .002, $P_{\text{TargetScan5}}$ = .005).

The upstream and downstream relationships of predicted mTOR targets to rapamycin-sensitive mTOR complex are shown in Fig. 4. From these 16 pre-selected microRNAs further prioritization was done according to high fold-changes in response to rapamycin as well as predicted targeting of central regulatory genes within mTOR pathway. Based on these criteria, the five miRNA-target pairs miR183-Tsc1, miR378-Tsc1, miR103-Pik3r1, miR107-Pik3r1 and miR182-Pik3r3 were subsequently selected for further evaluation.

3.4 Validation of miRNA-target gene interactions

To experimentally confirm *in silico* predicted miRNA-target gene pairs luciferase-based binding assays and transfection assays were performed. A significantly reduced luciferase activity strongly indicated binding of both miR-183 and -378 to the 3'UTR of their predicted target gene *Tsc1* (60.1 % *P*< .0001 and 27.0 % *P* = .001 respectively) and further of miR-103 to its predicted *Pik3r1* target gene 3'UTR (23.5 % P = .002; Fig. 5A). MiR-107 and -182 did not bind to *Pik3r1* and *Pik3r3* 3'UTR respectively (Fig. 5A).

To assess miRNA-mediated target gene regulation miRNA transfection assays were performed. Therefore cells were transfected with the respective candidate Pre-miR^{TM} miRNA Precursor molecules, leading to a strong up-regulation of the respective intracellular miRNA levels (data not shown). Indeed, target gene *Tsc1* expression was strongly down-regulated by miR-183 and -378 (18.3 % *P* = .004 and 40.4 % P < .0001 respectively). Likewise, miR-103 transfection resulted in significant down-regulation of *Pik3r1* levels (25.2 % *P*< .0001; Fig. 5B). MiR-107 and -182 did not alter *Pik3r1* and *Pik3r3* expression (Fig. 5B).

Taken together both, luciferase and transfection assay results validated *in silico* prediction of the miRNA-target pairs miR183-*Tsc1*, miR378-*Tsc1* and miR103-*Pik3r1*.

Table 1. mTOR target prediction of rapamycin-sensitive miRNAs. MiRNAs with confirmed differential expression on day 8 of differentiation in the presence or absence of rapamycin were subjected to target prediction

microRNA	rapamycin effect*	Predicted mTOR pathway target genes
miR-182	**-3.06**	***Mapk1, Pik3r3, Rictor***
miR-96	-2.90	*Akt3, mTOR, Rptor, Rictor, Rps6ka6*
miR-183	**-2.70**	***Rps6ka2, Tsc1***
miR-378	**-2.12**	***Akt1, Mapk1, Cab39, Tsc1***
miR-103/107	**-1.66/-2.10**	***Eif4b, Cab39, Pik3cb, Pik3r1, Vegfa***
miR-143	-0.83	*Eif4b, Pik3cg, Pik3r3, Rps6ka1, Rps6ka2*
miR-30a	-0.82	*Prkaa2, Cab39, Pik3cd, Pik3r2, Ddit4, Rictor, Rps6kb1*
miR-494	-0.76	*Akt1, Akt3, Prkaa2, Ulk2, Igf1, Mapk1, Cab39, Pik3cb*
miR-340-5p	-0.72	*Akt3, Hif1a, Igf1, Rps6kb1*
miR-29a	0.65	*Akt3, Eif4e2, Igf1, Pik3cg, Pik3r1, Pik3r3, Rptor, Vegfa*
miR-503	1.01	*Akt3, Eif4b, Eif4e, Rictor, Vegfa*
miR-125b-5p	1.03	*Eif4ebp1, Rps6ka1, Vegfa*
miR-199a-3p	1.06	*Hif1a, mTOR, Pik3cd, Rheb, Rps6kb1*
miR-214	1.06	*Akt2, Akt3, Ulk1, Eif4b, Igf1, Cab39, Pik3cb, Pik3r3, Rictor, Rps6ka1, Vegfa*
miR-222	1.61	*Prkaa2, Pik3r1, Ddit4, Rps6kb1, Tsc2*

**Rapamycin effect: log_2 fold change (day 8 rapamycin treatment - day 8)*

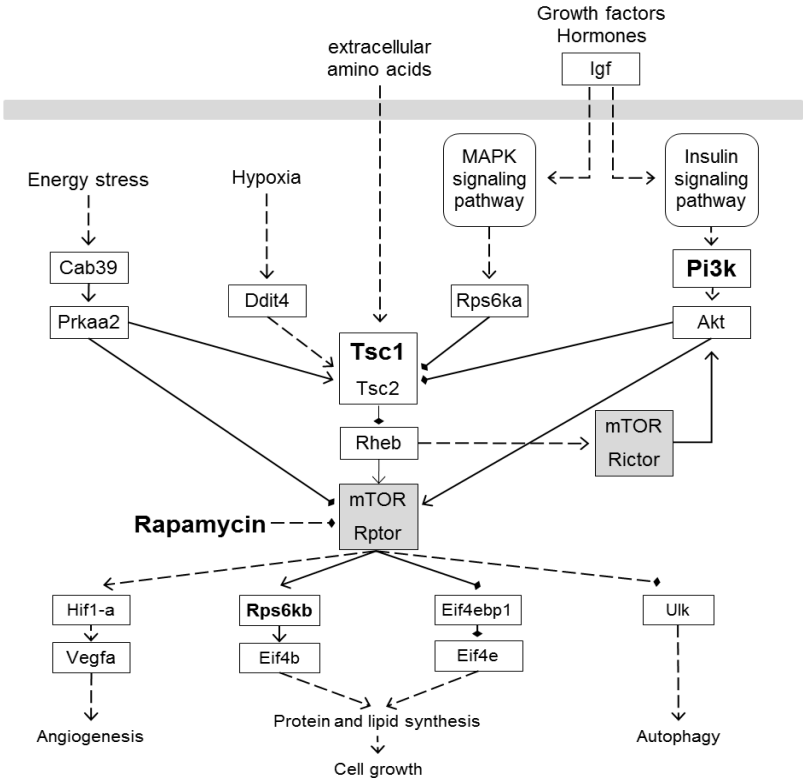

Fig. 4. Scheme of predicted miRNA targets within mTOR signaling pathway

→ molecular interaction or activation, —♦ inhibition, ⇢ indirect effect. Genes from mTOR target prediction (Table 1) are depicted. Pik3r1 and Pik3r3 genes encode two different regulatory subunits of Pi3k. MiRNA targets Tsc1, Pik3r1 and Pik3r3 were further investigated. Rps6kb gene encodes S6k1 protein

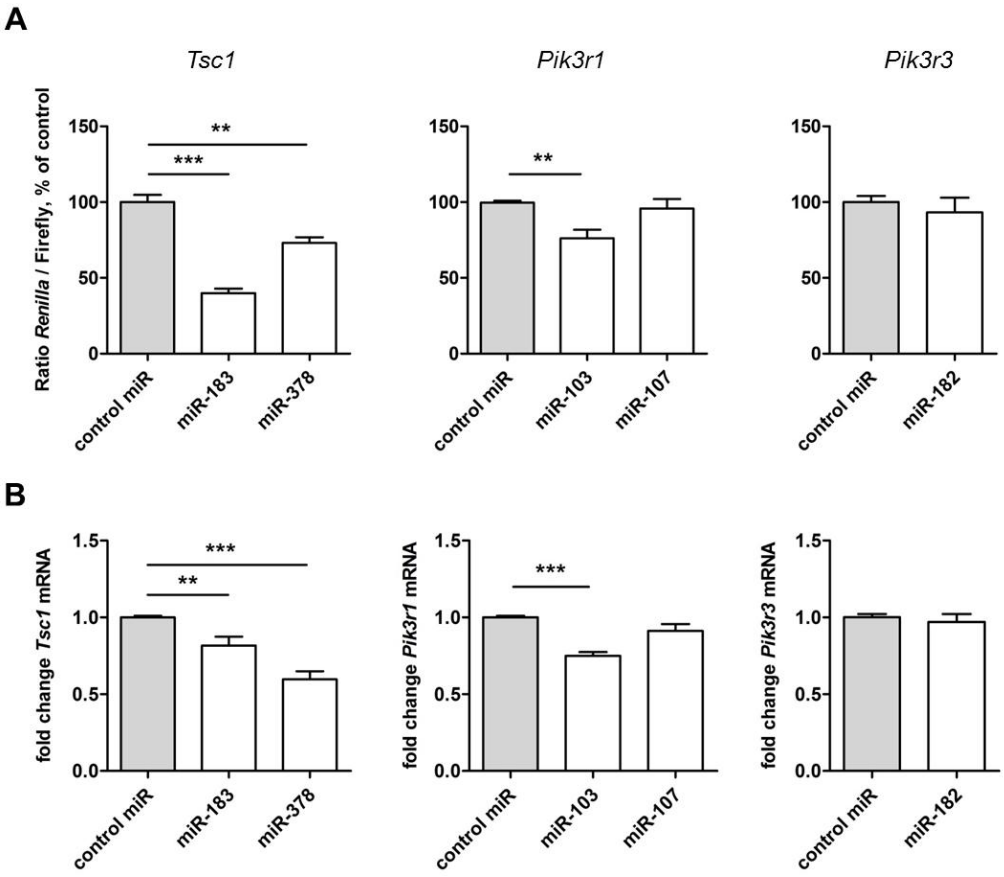

Fig. 5. Validation of miRNA-target gene interactions. (A) Experimental confirmation of miRNA binding to the 3'UTR of the predicted target genes by luciferase reporter assays. Relative luciferase activity of HEK-293 cells transfected with miR-183, -378, -103, -107 and -182 and a luciferase reporter plasmid harbouring the 3'UTRs of the respective target mRNAs are given. (B) Confirmation of target gene down-regulation after miRNA transfection. Gene expression levels of *Tsc1*, *Pik3r1* and *Pik3r3* were quantified using real-time PCR 3 days after transfection of 3T3-L1 cells with the respective miRNA and control molecules

(A) Mean values ± S.E.M. of two independent experiments each performed in triplicates
*(B) Mean values ± S.E.M. of four independent experiments. ** P ≤ .01, *** P ≤ .001*

3.5 miRNA-mediated functional effects

The functional relevance of the candidate miRNAs was further evaluated by measuring miRNA-mediated effects on target protein levels, mTOR signaling and adipocyte differentiation. To our surprise transfection of 3T3-L1 pre-adipocytes with miR-183 and -378 led to a slight increase in Tsc1 protein levels (35.7 % *P* = .29 and 39.8 % P = .49; Fig. 6A and B), whereas both miRNAs have been shown to decrease *Tsc1* gene expression (Fig. 5B). These results suggest complex regulation mechanisms of mTOR signaling. Pik3r1 protein levels did not change in cells transfected with miR-103 or -107 (Fig. 6A and B).

Based on previous reports that mTORC1 regulates protein synthesis *via* phosphorylation of p70 S6k1 protein encoded by the *Rps6kb* gene ([30], Fig. 4), miRNA effects on mTOR signaling were evaluated by measuring S6k1 phosphorylation. Fig. 6C and D show a moderate decrease in Phospho-S6k1 levels relative to total S6k1 protein levels in cells transfected with miR-183 and -378 (33.6 % *P* = .10 and 32.9 % *P* = .28). This may point to miRNA-mediated attenuation of mTOR signaling, whereas miR-103, -107 and -182 did not show an effect on S6k1 phosphorylation.

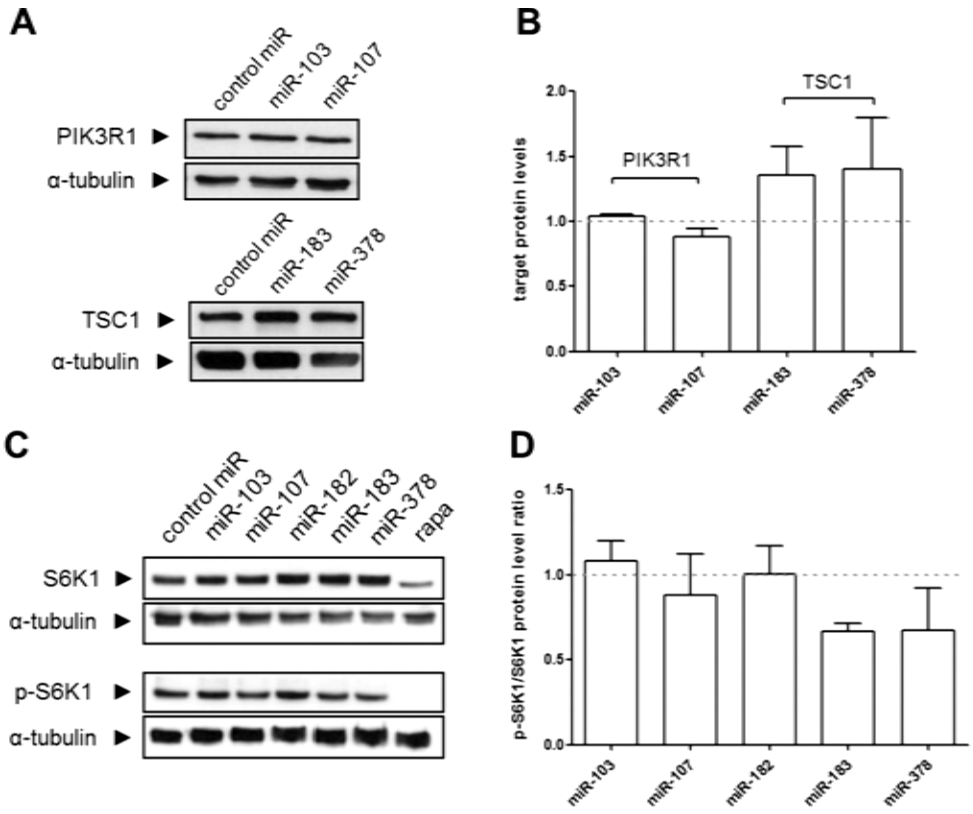

Fig. 6. Functional effects of candidate miRNAs on mTOR signaling. (A), (C) MiRNA effects on target protein levels and S6k1 phosporylation. Immunoblots of Pik3r1 (P85A), Tsc1 (hamartin), S6k1 and p-S6k1 protein in cells transfected with miR-103, -107, -182, -183 or -378. α-tubulin was used as loading control. (B), (D) Densitometric analysis of immunoblots. p-S6k1 levels are presented as p-S6k1/S6k1 quotient

(B), (D) Immunoblots from 2 independent experiments, each presented as relative ratio of the respective protein levels to α-tubulin relative to control treatments

Functional effects of miR-183 and -378 on adipocyte differentiation were evaluated in differentiation assays. During normal cell differentiation and in the absence of rapamycin miR-378 levels increased continuously from day 2 on, whereas miR-183 levels showed a sharp increase from day 6 on (Fig. 7A and B). In a second approach 3T3-L1 cells were transfected with anti-miR-183 and -378 resulting in a strong intracellular miRNA level reduction (data not shown) and differentiated for 6 days subsequently. Anti-miR-183 and -378 transfections led to an adipocyte marker gene *Ppar-γ* increase (38.5 % and 49.0 %) and pre-adipocyte marker gene *Dlk1* reduction in differentiated cells (42.5 % and 38.5 %; Fig. 7C). These results are consistent with the hypothesis that miR-183 and -378 attenuate mTOR-signaling and adipocyte differentiation.

4. DISCUSSION

In this study we aimed at identifying a subset of miRNAs being involved in adipocyte differentiation *via* regulation of the mTOR pathway. Our strategy for miRNA discovery included utilization of two different miRNA microarray platforms, which produced comparable results with reasonable good correlation as described previously [31]. Only those miRNAs were considered as confirmed which showed corresponding deregulation both in semiquantitative screening and quantitative confirmatory microarray. This strategy proved to be highly efficient even though few differentially expressed miRNAs may be lost because not all miRNAs were present on both platforms.

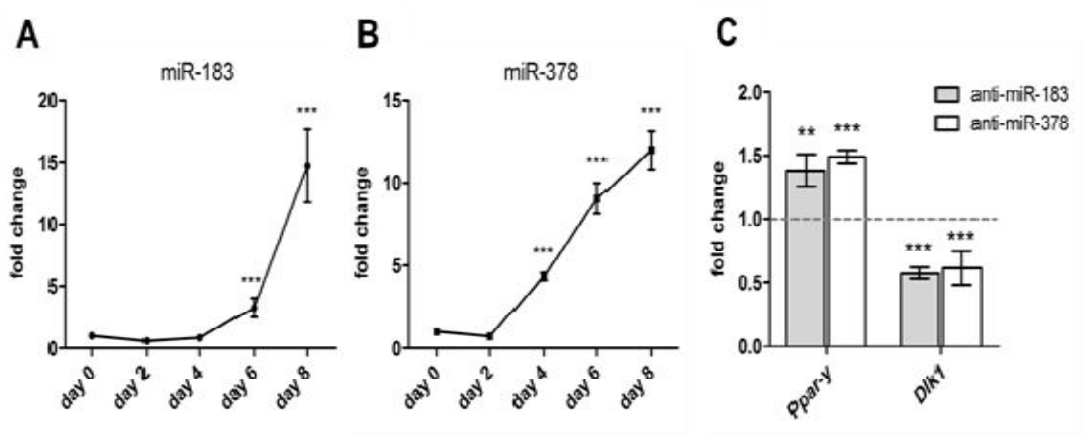

Fig. 7. Expression changes of (A) miR-183 and (B) miR-378 during 8 days of differentiation. (C) Effects of candidate miRNAs on adipocyte and pre-adipocyte markers. Real-time PCR mediated quantification of adipocyte marker *Ppar-γ* and pre-adipocyte marker *Dlk1* (alias *Pref-1*) in cells which were differentiated for 6 days after transfection with anti-miR-183 and -378 normalized to control cells. For both miRNAs and biomarker levels normalized fold changes are shown

Mean values ± S.E.M of two independent experiments, each measured in triplicates.
*** P ≤ .01 *** P ≤ .001 (A, B) Asterisks show significant regulation as compared to day 0.*
(C) Changes were significant in both experiments

We initially identified 40 miRNAs as differentially regulated during 3T3-L1 differentiation (day 0 – day 8) in the absence of any pharmacological alteration of the mTOR pathway. These results were consistent with earlier studies reporting 31 of these differentially regulated miRNAs, that appear to be involved in regulating fat cell differentiation in adipocyte cell lines derived from humans and mice [13,15,32]. Discrepant results compared to prior knowledge were only observed for expression levels of two miRNAs, miR-27b [33] and miR-182 [34]. Beyond this prior knowledge, our study additionally revealed differential regulation of miR-34a, -96, -106b, -148b, -678, -690 and -214*, all of them not yet being documented in the context of fat cell differentiation. Some of these miRNAs have been implicated in insulin signaling or glucose metabolism, such as miR-96 or miR-690 [35,36] or in cell cycle regulation, such as miR-96, miR-106b or miR-34a [37-42]. Cluster miR-183-96-182, which we found markedly deregulated during adipocyte differentiation, has previously been described to play an important role in the control of signal transductions by targeting 12 different signaling pathways, including insulin signaling [35].

MiRNAs, whose expression is significantly altered during differentiation, must be expected to arise as a consequence of regulatory events occurring in numerous pathways that can govern adipogenesis [43]. The specific aim of this study was to identify those involved in mTOR signaling, one of the key nutrient sensing pathways. Our study confirmed the inhibitory effect of rapamycin on adipocyte differentiation as evidenced by quantification of marker transcripts and decreased deposition of lipid droplets [3,44,45]. In the absence of mTOR inhibitor rapamycin *Ppary* expression showed a continuous increase throughout differentiation. This transcription factor trans-activates the expression of adipocyte-specific genes involved in glucose and lipid metabolism and thus plays a critical role in the induction of adipocyte differentiation as well as for maintenance of the mature adipocyte phenotype [46]. In contrast, transmembrane protein Dlk1 has already been described as an adipocyte differentiation inhibitor [46]. The protein is involved in maintaining the pre-adipocyte phenotype and thus its down-regulation is required for adipose conversion. Accordingly transcript levels of *Dlk1* showed a sharp decrease in the early stage of 3T3-L1 differentiation and disappeared later on. Addition of rapamycin reversed such physiological regulation of differentiation marker transcripts which is suggestive for a central role of mTOR in nutrient driven adipocyte differentiation. Additionally, chronic mTOR inhibition attenuated regulation of differentiation-associated miRNAs.

Almost half of the miRNAs (18 out of 40) differentially regulated during adipogenesis were also sensitive to rapamycin-treatment. MiR-340-5p, -494, -322 and -450a-5p were identified as 'rapamycin-sensitive', though showing no differential regulation during adipogenesis. Aside from miR-322, which has been described as regulator of adipogenesis *via* the WNT/ß catenin signaling pathway in another study [47], these miRNAs may mediate differentiation-independent effects of mTOR signaling.

Although the miRNA pattern involved in mTOR signaling during adipocyte differentiation has not yet been elucidated, members of miR-99 family (miR-99a and -b, miR-100) and miR-199a-3p have been implicated in mTOR signaling in other biological settings [17-20]. Accordingly we identified miR-199a-3p as rapamycin-sensitive, whereas miR-100 slightly missed our criterion of adj $P< .05$ (adj $P_{miR-100} = .08$) and miR-99a and -b were not deregulated at all in our adipocyte study.

To identify presumptive miRNA-target pairs within the mTOR pathway, our set of 22 'rapamycin-sensitive' miRNAs was subjected to a stringent *in silico* target prediction. Among these, 16 were indeed predicted to target components of the mTOR pathway, thereby confirming the utility of rapamycin in the experimental discovery approach. Moreover, mTOR pathway targets were found to be significantly enriched in the set of predicted rapamycin-sensitive miRNA targets. Our analyses included all mTOR pathway genes, up- and downstream of mTOR complex 1, the site of rapamycin action, and thus may comprise miRNAs functionally involved in regulatory loops [48].

Subsequently we selected five 'rapamycin-sensitive' miRNAs for further studies and confirmed physical interaction of the three predicted miRNA-target gene pairs miR183-*Tsc1*, miR378-*Tsc1* and miR103-*Pik3r1* by luciferase reporter assays. Additionally, transfection assays confirmed miRNA miR-183, -378 and -103 mediated down-regulation of the respective target transcripts *Tsc1* and *Pik3r1*. However, immunoblots of Tsc1 protein levels show that these are inversely correlated with the respective target mRNA levels in cells transfected with miR-183 and -378. This unexpected phenomenon could be due to functionally overruling regulation of up-stream targets resulting in de-regulated protein levels in the whole signaling cascade. Tsc1 is known to inhibit mTOR [49] and in line with that, we found decreased mTOR signaling on a functional level. This effect was associated with an inhibitory effect on adipocyte differentiation as anti-miR-183 and -378 treatments led to increased adipocyte marker and decreased pre-adipocyte marker gene expression. Therefore, these miRNAs seem to attenuate both mTOR signaling and differentiation. The different shape in the time-course of these miRNAs during differentiation suggests that miR-183 may rather play a role only in the late phase of differentiation while miR-378 appears to be functional also in earlier phases.

As one limitation of this study the entire network and time-course of regulation in mTOR pathway by the proposed candidate miRNAs is not yet fully characterized. This would e.g. need functional experiments for mTOR signaling activation both in miR-183 and -378 overexpressing cells and controls. Gene expression data from such cells might reveal the regulatory network of the candidate miRNAs beyond Tsc in more detail.

5. CONCLUSION

Taken together, this study identified a subset of miRNAs playing both a role in mTOR signaling and in adipocyte differentiation. In particular we showed that miR-183 and -378 are functionally relevant in adipocyte differentiation *via* influence on mTOR signaling. They could potentially serve as biomarkers for nutrient-driven dysregulation of adipogenesis.

COMPETING INTERESTS

Authors have declared that no competing interests exist.

REFERENCES

1. Marshall S. Role of insulin, adipocyte hormones, and nutrient-sensing pathways in regulating fuel metabolism and energy homeostasis: a nutritional perspective of diabetes, obesity, and cancer. Sci STKE. 2006;2006:re7.
2. Chakrabarti P, English T, Shi J, Smas CM, Kandror KV. Mammalian target of rapamycin complex 1 suppresses lipolysis, stimulates lipogenesis, and promotes fat storage. Diabetes. 2010;59:775-81.

3. Cho HJ, Park J, Lee HW, Lee YS, Kim JB. Regulation of adipocyte differentiation and insulin action with rapamycin. Biochem Biophys Res Commun. 2004;321:942-8.
4. Um SH, D'Alessio D, Thomas G. Nutrient overload, insulin resistance, and ribosomal protein S6 kinase 1, S6K1. Cell Metab. 2006;3:393-402.
5. Birse RT, Choi J, Reardon K, Rodriguez J, Graham S, Diop S, et al. High-fat-diet-induced obesity and heart dysfunction are regulated by the TOR pathway in Drosophila. Cell Metab. 2010;12:533-44.
6. Johnston O, Rose CL, Webster AC, Gill JS. Sirolimus is associated with new-onset diabetes in kidney transplant recipients. J Am Soc Nephrol. 2008;19:1411-8.
7. Teutonico A, Schena PF, Di Paolo S. Glucose metabolism in renal transplant recipients: effect of calcineurin inhibitor withdrawal and conversion to sirolimus. J Am Soc Nephrol. 2005;16:3128-35.
8. Yang SB, Lee HY, Young DM, Tien AC, Rowson-Baldwin A, Shu YY, et al. Rapamycin induces glucose intolerance in mice by reducing islet mass, insulin content, and insulin sensitivity.J Mol Med (Berl). 2012;90:575-85.
9. Deblon N, Bourgoin L, Veyrat-Durebex C, Peyrou M, Vinciguerra M, Caillon A, et al. Chronic mTOR inhibition by rapamycin induces muscle insulin resistance despite weight loss in rats. Br J Pharmacol. 2012;165:2325-40.
10. Zahr E, Molano RD, Pileggi A, Ichii H, San Jose S, Bocca N, et al. Rapamycin impairs beta-cell proliferation in vivo. Transplant Proc. 2008;40:436-7.
11. Sacco J, Adeli K. MicroRNAs: emerging roles in lipid and lipoprotein metabolism. Curr Opin Lipidol. 2012;23:220-5.
12. Lim LP, Lau NC, Garrett-Engele P, Grimson A, Schelter JM, Castle J, et al. Microarray analysis shows that some microRNAs downregulate large numbers of target mRNAs. Nature. 2005;433:769-73.
13. Alexander R, Lodish H, Sun L. MicroRNAs in adipogenesis and as therapeutic targets for obesity. Expert Opin Ther Targets. 2011;15:623-36.
14. Heneghan HM, Miller N, Kerin MJ. Role of microRNAs in obesity and the metabolic syndrome. Obes Rev. 2009;11:354-61.
15. McGregor RA, Choi MS. microRNAs in the regulation of adipogenesis and obesity. Curr Mol Med. 2011;11:304-16.
16. Esau C, Davis S, Murray SF, Yu XX, Pandey SK, Pear M, et al. miR-122 regulation of lipid metabolism revealed by in vivo antisense targeting. Cell Metab. 2006;3:87-98.
17. Doghman M, El Wakil A, Cardinaud B, Thomas E, Wang J, Zhao W, et al. Regulation of insulin-like growth factor-mammalian target of rapamycin signaling by microRNA in childhood adrenocortical tumors. Cancer Res. 2010;70:4666-75.
18. Nagaraja AK, Creighton CJ, Yu Z, Zhu H, Gunaratne PH, Reid JG, et al. A link between mir-100 and FRAP1/mTOR in clear cell ovarian cancer. Mol Endocrinol. 2010;24:447-63.
19. Fornari F, Milazzo M, Chieco P, Negrini M, Calin GA, Grazi GL, et al. MiR-199a-3p regulates mTOR and c-Met to influence the doxorubicin sensitivity of human hepatocarcinoma cells. Cancer Res. 2010;70:5184-93.
20. Jin Y, Tymen SD, Chen D, Fang ZJ, Zhao Y, Dragas D, et al. MicroRNA-99 Family Targets AKT/mTOR Signaling Pathway in Dermal Wound Healing. PLoS One. 2013;8:e64434.
21. Green H, Kehinde O. Sublines of Mouse 3t3 Cells That Accumulate Lipid. Cell. 1974;1:113-6.
22. Pfaffl MW. A new mathematical model for relative quantification in real-time RT-PCR. Nucleic Acids Res. 2001;29:e45.
23. Papadopoulos GL, Alexiou P, Maragkakis M, Reczko M, Hatzigeorgiou AG. DIANA-mirPath: Integrating human and mouse microRNAs in pathways. Bioinformatics. 2009;25:1991-3.
24. Untergasser A, Nijveen H, Rao X, Bisseling T, Geurts R, Leunissen JA. Primer3Plus, an enhanced web interface to Primer3. Nucleic Acids Res. 2007;35:W71-4.
25. Gentleman RC, Carey VJ, Bates DM, Bolstad B, Dettling M, Dudoit S, et al. Bioconductor: open software development for computational biology and bioinformatics. Genome Biol. 2004;5:R80.
26. Smyth GK, Michaud J, Scott HS. Use of within-array replicate spots for assessing differential expression in microarray experiments. Bioinformatics. 2005;21:2067-75.
27. Ritchie ME, Silver J, Oshlack A, Holmes M, Diyagama D, Holloway A, et al. A comparison of background correction

methods for two-colour microarrays. Bioinformatics. 2007;23:2700-7.
28. Smyth GK. Linear models and empirical bayes methods for assessing differential expression in microarray experiments. Stat Appl Genet Mol Biol. 2004;3:Article3.
29. Benjamini Y, Hochberg Y. Controlling the False Discovery Rate - a Practical and Powerful Approach to Multiple Testing. Journal of the Royal Statistical Society Series B-Methodological. 1995;57:289-300.
30. Tee AR, Blenis J. mTOR, translational control and human disease. Semin Cell Dev Biol. 2005;16:29-37.
31. Wang B, Howel P, Bruheim S, Ju J, Owen LB, Fodstad O, et al. Systematic evaluation of three microRNA profiling platforms: microarray, beads array, and quantitative real-time PCR array. PLoS One. 2011;6:e17167.
32. Romao JM, Jin W, Dodson MV, Hausman GJ, Moore SS, Guan le L. MicroRNA regulation in mammalian adipogenesis. Exp Biol Med (Maywood). 2011;236:997-1004.
33. Ortega FJ, Moreno-Navarrete JM, Pardo G, Sabater M, Hummel M, Ferrer A, et al. MiRNA expression profile of human subcutaneous adipose and during adipocyte differentiation. PLoS One. 2010;5:e9022.
34. Sun T, Fu M, Bookout AL, Kliewer SA, Mangelsdorf DJ. MicroRNA let-7 regulates 3T3-L1 adipogenesis. Mol Endocrinol. 2009;23:925-31.
35. Xu J, Wong C. A computational screen for mouse signaling pathways targeted by microRNA clusters. RNA. 2008;14:1276-83.
36. Tang X, Muniappan L, Tang G, Ozcan S. Identification of glucose-regulated miRNAs from pancreatic {beta} cells reveals a role for miR-30d in insulin transcription. RNA. 2009;15:287-93.
37. Guttilla IK, White BA. Coordinate regulation of FOXO1 by miR-27a, miR-96, and miR-182 in breast cancer cells. J Biol Chem. 2009;284:23204-16.
38. Myatt SS, Wang J, Monteiro LJ, Christian M, Ho KK, Fusi L, et al. Definition of microRNAs that repress expression of the tumor suppressor gene FOXO1 in endometrial cancer. Cancer Res. 2010;70:367-77.
39. Petrocca F, Vecchione A, Croce CM. Emerging role of miR-106b-25/miR-17-92 clusters in the control of transforming growth factor beta signaling. Cancer Res. 2008;68:8191-4.
40. Ivanovska I, Ball AS, Diaz RL, Magnus JF, Kibukawa M, Schelter JM, et al. MicroRNAs in the miR-106b family regulate p21/CDKN1A and promote cell cycle progression. Mol Cell Biol. 2008;28:2167-74.
41. Sun F, Fu H, Liu Q, Tie Y, Zhu J, Xing R, et al. Downregulation of CCND1 and CDK6 by miR-34a induces cell cycle arrest. FEBS Lett. 2008;582:1564-8.
42. Hermeking H. The miR-34 family in cancer and apoptosis. Cell Death Differ. 2010;17:193-9.
43. MacDougald OA, Lane MD. Transcriptional regulation of gene expression during adipocyte differentiation. Annu Rev Biochem. 1995;64:345-73.
44. Kim JE, Chen J. regulation of peroxisome proliferator-activated receptor-gamma activity by mammalian target of rapamycin and amino acids in adipogenesis. Diabetes. 2004;53:2748-56.
45. Yeh WC, Bierer BE, McKnight SL. Rapamycin inhibits clonal expansion and adipogenic differentiation of 3T3-L1 cells. Proc Natl Acad Sci U S A. 1995;92:11086-90.
46. Gregoire FM, Smas CM, Sul HS. Understanding adipocyte differentiation. Physiol Rev. 1998;78:783-809.
47. Qin L, Chen Y, Niu Y, Chen W, Wang Q, Xiao S, et al. A deep investigation into the adipogenesis mechanism: profile of microRNAs regulating adipogenesis by modulating the canonical Wnt/beta-catenin signaling pathway. BMC Genomics. 2010;11:320.
48. Efeyan A, Sabatini DM. mTOR and cancer: many loops in one pathway. Curr Opin Cell Biol. 2010;22:169-76.
49. Huang J, Manning BD. The TSC1-TSC2 complex: a molecular switchboard controlling cell growth. Biochem J. 2008;412:179-90.

APPENDIX

Table s1. Differentially regulated miRNAs during adipogenesis. miRNAs with confirmed (a) up-regulation or (b) down-regulation in differentiated adipocytes (day 8) compared to pre-adipocytes (day 0) are depicted

A			B		
microRNA	**log_2FC (d8/d0)***	**adj *P*-value**	**microRNA**	**log_2FC (d8/d0)***	**adj *P*-value**
miR-378	3.05	4.85E-07	*miR-222*	-1.68	1.49E-06
miR-193	3.03	6.18E-11	*miR-221*	-1.62	3.05E-03
miR-107	2.87	1.49E-06	*miR-34c*	-1.46	9.50E-05
miR-103	2.84	1.49E-06	*miR-214*	-1.24	8.81E-05
miR-210	2.64	6.27E-04	*miR-214**	-1.18	3.49E-02
miR-146b	2.40	1.49E-06	*miR-34a*	-1.01	3.04E-05
miR-365	2.35	8.19E-03	*miR-29a*	-0.94	1.13E-04
miR-96	1.75	3.86E-05	*miR-199b**	-0.84	6.27E-04
miR-183	1.46	7.29E-03	*miR-678*	-0.82	3.44E-03
miR-182	1.21	1.28E-02	*miR-199a-5p*	-0.77	4.95E-04
miR-143	1.12	1.16E-04	*miR-31*	-0.77	1.29E-03
miR-22	1.10	6.27E-04	*miR-199a-3p*	-0.73	6.10E-04
miR-30a	1.07	1.75E-04	*miR-503*	-0.67	1.63E-03
miR-148b	1.02	3.92E-02	*miR-125a-5p*	-0.63	5.74E-03
let-7c	0.89	8.17E-04	*miR-125b-5p*	-0.60	3.79E-03
miR-30c	0.85	1.17E-03	*miR-690*	-0.45	3.92E-02
miR-30e	0.83	2.28E-03			
miR-152	0.83	5.69E-03			
miR-10b	0.80	5.76E-03			
miR-15a	0.75	4.21E-02			
miR-106b	0.64	3.09E-02			
miR-30b	0.61	7.59E-03			
let-7d	0.50	3.52E-02			
miR-27b	0.35	4.42E-02			

**FC: fold change, d8: day 8, d0: day 0*

Peer-review history:
The peer review history for this paper can be accessed here:
http://www.sciencedomain.org/review-history.php?iid=875&id=39&aid=7373